Proceedings of the ASME 2010 3rd Joint US-European Fluids Engineering Summer Meeting and 8th International Conference on Nanochannels, Microchannels, and Minichannels
FEDSM-ICNMM2010
August 1-5, 2010, Montreal, Canada

FEDSM-ICNMM2010-30179

ON THE HEAT TRANSFER CHARACTERISTICS OF HIGHLY COMPACT HEAT SINKS

Chi-Chuan Wang
ccwang@mail.nctu.edu.tw
Department of Mechanical Engineering, National Chiao Tung University,
Hsinchu, Taiwan 300

ABSTRACT

This study conducts an experimental study concerning the airside performance of highly compact heat sinks under cross flow condition. The test fin patterns can be classified into four categories, namely the base plain fin heat sink (Type I), interrupted fin geometry (Type II), dense vortex generator (Type III), loose vortex generator (Type IV) and their combinations. It is found that the heat transfer performance is strongly related to the arrangement of enhancements. The interrupted and dense vortex generator configurations normally contribute more pressure drop penalty than improvements of heat transfer. This deterioration becomes especially evident at a lower frontal velocity. The oblique VG with cannelure structure shows an appreciable lower pressure drop than that of plain fin geometry. In the meantime, the presence of interrupted surface may also jeopardize heat conduction path due to constriction. The results indicate that the vortex generators operated at a higher frontal velocity is more beneficial than that of plain fin geometry. In summary of the test results, it is therefore concluded that augmentation via various fin patterns like interrupted or vortex generator is quite effective only at developing region. However, the conventional enhanced fin patterns lose its superiority at the fully developed region. To tackle this problem, some techniques employing swing flow or unstable flow field accompanied with the asymmetric design, shows potential to resolve this problem.

Keywords: Electronic cooling, Heat sink, Vortex generator.

NOMENCLATURE

A	Heat transfer surface area (m^2)
A_c	Cross sectional area at the test section (m^2)
A_{front}	Frontal area of fins (m^2)
C	Perimeter of the rectangular section (m)
Cp_a	Specific heat at constant pressure of air (J kg^{-1} K^{-1})
D_h	Hydraulic diameter (m^2)
f	Friction factor (dimensionless)
F_s	Fin spacing (m)
$\bar{h}$	Average convective heat transfer coefficient (W m^{-2} K^{-1})
h_0	Effective heat transfer coefficient (W m^{-2} K^{-1})
j	Colburn factor (dimensionless)
H	Fin height (m)
H_b	Thickness of base plate (m)
L	Duct length (m)
k	The thermal conductivity of air (W m^{-1} K^{-1})
$\dot{m}$	mass flow rate (kg s^{-1})
N	Number of fins (dimensionless)
P	Fin perimeter (m)
Pr	Prandtl number. (dimensionless)
$\dot{Q}_{conv}$	Convention heat transfer rate (W)
Re_{D_h}	Duct Reynolds number (dimensionless)
T_{avg}	The average temperature of the air (K)
T_w	The average surface temperature (K)
V_c	The mean velocity in the flow channel (m s^{-1})
V_{front}	The frontal velocity (m s^{-1})
$\dot{V}$	Volumetric air flow rate (m^3 s^{-1})
x^+	Inverse Graetz number (dimensionless)

INTRODUCTION

With the advance of electronic products showing significant performance improvements and versatile capability, the associated heat generation is also being dramatically increased. Hence the risk of failure and performance loss is increasing for the electronic devices, and sometimes may lead to a system failure. Among the causes that lead to catastrophic of electronic system, over-temperature is regarded as the major cause of electronic failures [1], yet it significantly affects components reliability. Therefore, it is quite essential to have effective thermal management to maintain the operation temperature below certain threshold limit for electronic devices. There were many methods applicable to electronic cooling such as liquid cooling, air cooling, refrigeration, thermoelectric, and the like. Among them, air cooling is still the most popular one for its simplicity and low cost. One of the common arrangements of air cooling is via forced convection of the heat sink to dissipate heat from heat sources. Two most common fin patterns of the heat sink take the form as plate and pin fin. The major advantages of these fin patterns are easy machining, simple structure and low cost.

Despite air cooling features simplicity and low cost, the low thermal conductivity of air inevitably results in a very low heat transfer coefficient. As a consequence, the general approach for heat transfer improvement is via exploitation of smaller fin spacing to accommodate more fin surface. However, a limitation is imposed on this conventional approach when the fin spacing is small or when the operation speed is low. This is made clear from Yang et al. [2] who examined the thermal-hydraulic performance of heat sinks having plain, slit, and louver fin configurations. Their results indicated a significant drop of heat transfer performance at the low Reynolds number and at small fin spacing. This is because fully developed flow prevails. In this sense, one would resort to interrupted fin geometry to reduce the thermal resistance. The general concept is via periodical renewal of boundary layer. Unfortunately, as pointed out by Yang et al. [2] and Webb and Trauger [3], typical interrupted surfaces like louver fin shows appreciable degradation in low velocity region pertaining to the "duct flow" phenomenon. The appreciable level-off of the heat transfer coefficient at this low velocity region for the louver fin geometry had been reported by some investigators. For example, Davenport [4] and Achaichia and Cowell [5] had reported that the deterioration of heat transfer coefficients in the low velocities region from their test results of an automotive multi-louver fin surface. Webb and Trauger [3] found that at a low Reynolds number some of the air streams bypass the louvers and act as "duct flow" between the fin channels, giving rise to a lower *j* factor. Typical flow patterns subject to the influence of velocity for a louver fin geometry can be schematically shown in Fig. 1. In short, the improvement of heat transfer performance is rather small in the low frontal velocities region. In addition to this general argument from previous investigators, Yang et al. [2] found that there is another cause of this heat transfer degradation. Notice that the level-off occurs not only to the louver fin geometry but also to the slit and plate fin geometry. Notice that Shah and Sekulić [6] had attributed to this phenomenon as the "experimental error". However, the Yang et al. [2] suspects that it is a physical phenomenon. For further illustration of this phenomenon, one can examine the corresponding reciprocal of the inverse Graetz number x^+, which is defined as

$$x^+ = \frac{L/D_h}{\mathrm{Re}_{D_h}\,\mathrm{Pr}} \tag{1}$$

Where L is the streamwise duct length and Pr is the Prandtl number. The flow may be considered to be fully developed when $x^+ > 0.1$ [7]. For further comparison about the influence of developing flow on the heat transfer performance, their test results are plotted in terms *j* vs. the inverse Graetz number as shown in Fig. 2. The right hand side of the ordinate ($x^+ > 0.1$) denotes the flow region being fully developed whereas the region $x^+ < 0.1$ represents the developing region. By carefully examining the test results, Yang et al. [2] found out that the test results at the lower Reynolds number fall within the fully developed region where a considerable drop of heat transfer performance can be easily explained. In the meantime, the heat transfer performance in the developing region reveals a much better heat transfer performance. In summary of these two distinct heat transfer characteristics, resulting in a maximum phenomenon of *j* vs. Re_{D_h}. The maximum position corresponds roughly to the point separating the region of fully developed and developing. This is applicable to all the fin geometries tested by them. This is because that in low velocity region the highly interrupted surface like louver acts like a duct flow [3], therefore no considerable differences are shown. The results imply a difficult situation of heat transfer augmentation occurring at the low velocity having smaller fin spacing.

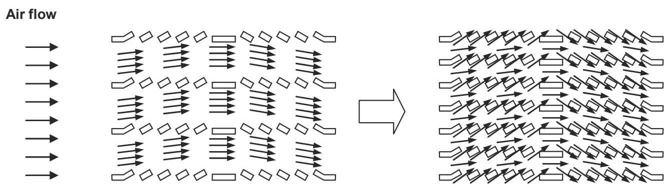

FIG. 1. SCHEMATIC OF DUCT FLOW VS. FIN-DIRECTED FLOW FOR LOUVER FIN GEOMETRY AT SMALLER and larger flow velocities.

The results imply a difficult situation of heat transfer augmentation occurring at a low velocity having smaller fin spacing. As explained earlier, the poor heat transfer performance is expected for its fully developed nature. Yet in the low Reynolds number region the interrupted surface suffers from the "duct flow" phenomenon. In summary of the foregoing results, it is found that significant augmentation is hard to achieve in this region (small fin spacing and low Reynolds number). One of the alternatives to tailor this problem is to introduce swirl flow and destabilized flow field, and the common way for doing this is using vortex generators [8] or dimple/protrusion structure [9].

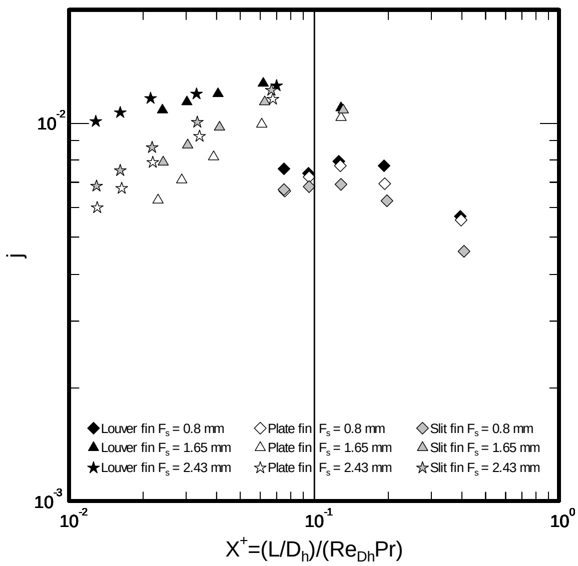

FIG. 2. INVERSE GRAETZ NUUMBER nUMBER X^+ vs. *J* for loUVER, SLIT AND PLATE FIN.

Vortex generators in early research were used to delay boundary layer separation on aircraft wings [10]. Recently, vortex generator is adopted for electronic cooling and the like because it reveals great potential in reducing the thermal resistance. However, the enhancements of heat transfer usually exceed pressure drop penalty. For example, Gentry and Jacobi [11] reported the average heat transfer enhancement of 20-50% with corresponding pressure drop penalty being approximately 50-110% for using vortex generators. The influence of dimple vortex generators depends on the arrangements of the dimple configuration, and the heat transfer rates and friction factors for dimpled channels are about 1.15–2.5 and 1.08–3.5 times higher than those of the smooth channel, respectively [12].

In practice, the electronic cooling applications often use very dense fin for heat dissipation due to space limitation. Unfortunately, the dense fin arrangements lead to early fully developed flow and results in a lower heat transfer performance occurring at low Reynolds number region. In the situation, it is hard to have a significant augmentation. Though some studies had been conducted for heat transfer enhancements for electronic cooling system, the information about augmented heat transfer performance at affordable pressure drop penalty especially at lower Reynolds number region is still quite demanding. Hence the purpose of the present study is to provide some recent efforts of various enhancements on the overall performance pertaining to electronic cooling applications. Efforts are made toward sufficient enhancements at an affordable pressure drop penalty.

EXPERIMENTAL APPARATUS

The experiment apparatus is based on ASHRAE wind tunnel setup to measure the heat transfer and the pressure drop characteristics of the heat sinks. Two main parts of the experimental apparatus are described in the following.

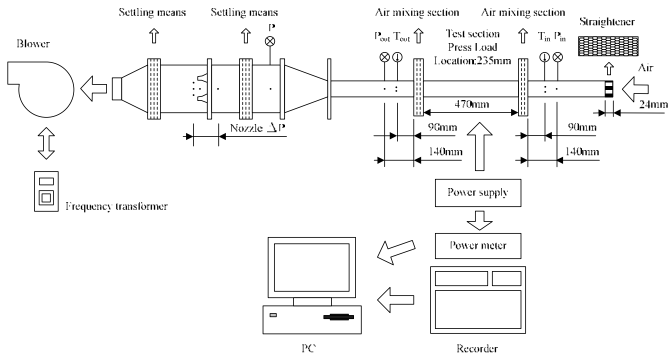

Fig. 3. Experimental setup.

TABLE 1 PHOTOS OFNTHE TEST HEAT SINKS.

Heat sink	Photos of test sample
(a) Plate	
(b) Delta VG	
(c) Delta VG+Plate	
(d)Semi-circular VG	
(e) Triangular VG	
(f) Triangular attack VG	
(g) Dimple VG	
(h)Two groups dimple VG	
(i) Oblique dimple gap (2-12) VG	
(j) Oblique dimple gap (4-12) VG	
(k) Oblique dimple gap (6-12) VG	
(l) Oblique dimple gap (6-12) cannelure VG	

Wind Tunnel

As seen in Fig. 3, experiments were performed in an open type wind tunnel. The ambient air flow was forced across the test section by a centrifugal fan with an inverter. To avoid and minimize the effect of flow mal-distribution in the experiments, an air straightener-equalizer and a mixer were provided. The inlet and the exit temperatures across the sample were measured by two T-type thermocouple meshes. The inlet measuring mesh consists of four thermocouples while the outlet mesh contains eight thermocouples. The sensor locations inside the rectangular duct were established following ASHRAE [13] recommendation. These data signals were individually recorded and then averaged. During the isothermal test, the variation of these thermocouples was within 0.2 °C. In addition, all the thermocouples were pre-calibrated by a quartz thermometer having 0.01 °C precision. The accuracies of the calibrated thermocouples are of 0.1 °C. The pressure drop of the test sample and nozzle was detected by a precision differential pressure transducer, reading to 0.1 Pa. The air flow measuring station was a multiple nozzle code tester based on the ASHRAE 41.2 standard [14]. All the data signals are collected and converted by a data acquisition system (a hybrid recorder). The data acquisition system then transmitted the converted signals through Ethernet interface to the host computer for further operation.

Heat Sink

A total of twelve heat sinks were made and tested, the corresponding fin patterns are (a) plain fin; (b) delta vortex generators fin; (c) delta vortex generators + plain fin (d) semi-circular vortex generators fin; (e) triangular vortex generators fin (f) triangular attack vortex generators; (g) dimple vortex generators fin (h) two-groups dimple vortex generators; (i) oblique dimple group with 2 mm distance from entrance to the first group dimple and 12 mm distance between the first and second group; (j) oblique dimple group with cannelure structure. For comparison purpose, experimental results of louver and slit fin form Yang et al. [3] are also included. The delta vortex generators are of equilateral triangle. The heat sinks are made from copper with a thermal conductivity of 398 W/m·K. The fabricated vortex generators are punched from copper sheet, leaving holes alongside the fin. Photos of the test heat sink are tabulated in Table 1. The base plates of the heat sinks are of square configuration with a length of 50 mm. The corresponding fin pitches is 1.0 mm with a constant fin thickness of 0.2 mm. In addition, the height of the heat sinks is 10 mm. A film heater with the same size of base plate is attached to the bottom of heat sink. During the tests, electric power supply provided 25 W power input to the heater. Five temperature sensors were placed below the heat sink to measure the average temperature of the heat sink. The bakelite board is installed beneath the film heater in order to minimizing the heat loss. The heat sinks were loaded to a constant force of 11 N for all experiment. This provided consistent thermal contact resistance between the heat sinks and heater.

ANALYSIS OF HEAT SINK

The airside performance of the test heat sinks are in terms of pressure drop and heat transfer performance characteristics. For determination of the friction factor of the test samples, an adiabatic test is performed to obtain the total pressure drops. Hence, the measured friction factor can be obtained from the following equation:

$$f = \frac{\Delta P}{4\left(\frac{L}{D_h}\right)\cdot\left(\frac{\rho V_c^2}{2}\right)} \tag{2}$$

Where L, D_h, and ρ are the duct length, hydraulic diameter and density of air. The hydraulic diameter (D_h) is defined by height of fin (H) and fin spacing (F_s), and can be obtained from the following equation:

$$D_h = \frac{4A_c}{P} = \frac{4\times\left(H\times F_s\right)}{2\times(H+F_s)} \tag{3}$$

The characteristic velocity is calculated by flow rate and cross sectional area at the test section as:

$$V_c = \frac{\dot{V}}{A_{ct} - A_{front}} \tag{4}$$

Where $\dot{V}$, A_{ct}, and A_{front} represent the volumetric flow rate, cross sectional area at the test section and the frontal area of the heat sink. The total heat transfer surface area (A) is the surface in contact with work fluid, and the cross sectional area at the test section of fin (A_{ct}) is the whole flow channel of test section can be calculated as:

$$A_{ct} = W \times H \tag{5}$$

The frontal area of fins (A_{front}) can calculate by Number of fins (N), thickness of fin (t) and height of fin (H) as flow:

$$A_{front} = N \times t \times H \tag{6}$$

The convective heat transfer rate of experimental system can be obtained from the following equation:

$$\dot{Q}_{conv} = \dot{m}Cp_a\left(T_{air,out} - T_{air,in}\right) \tag{7}$$

Where $\dot{m}$, Cp_a, $T_{air,out}$ and $T_{air,in}$ represent mass flow rate, specific heat, average temperature of the inlet test section and the average temperature of the outlet test section.

The heat transfer coefficients are evaluated from the measured wall and air temperature:

$$\bar{h} = \frac{\dot{Q}_{conv}}{A_{plate}\left(T_w - T_{air,avg}\right)} \tag{8}$$

Where T_w is the average surface temperature and T_{avg} is the average temperature of the air at the test section. The heat transfer performance can be in terms of dimensionless Colburn j factor as

$$j = \frac{h_o}{\rho V_c C p_a} \Pr^{2/3} \quad (9)$$

Uncertainties in the reported experimental values were estimated by the method suggested by Moffat [15]. The highest uncertainties are 3.71% for the heat transfer coefficient and 2.02% for f. The highest uncertainties were associated with lowest Reynolds number.

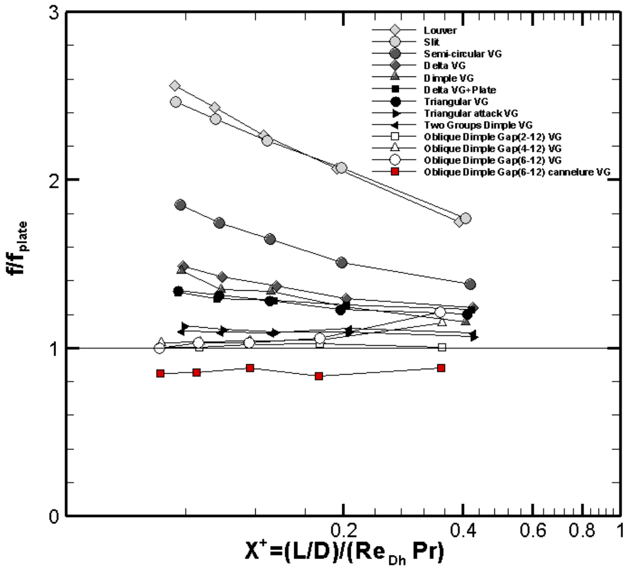

FIG. 4. INVERSE GRAETZ NUMBER X+ VS. f/f_{plain} FOR THE TEST HEAT SINKS.

RESULTS AND DISCUSSION

Normally the effective approach of heat transfer improvement (from $Q = hA\Delta T_m$, Q: total heat dissipated, A: area, h: convective heat transfer coefficient, ΔT_m: effective mean temperature difference) is via increase of heat dissipated area, improving convective heat transfer coefficient, or both. In this study, we have investigated various kinds of improvements characterizing the forgoing augmentations. The tested samples can be further divided into the following four categories.

Type I: Plate fin heat sink featuring heat transfer improvement from increasing heat dissipate surface. Generally, the general heat transfer augmentation is via smaller fin spacing to accommodate more fin surface.

Type II: Heat sink with interrupted fin geometry which improves convective heat transfer coefficient via periodical renewal of boundary layer and they take the form such as slit or louver fin.

Type III: Heat sink with dense vortex generator. The enhancements introduce swirl flow, Coanda deflection flow or destabilized flow field from vortex generators or dimple/protrusion structure. The general arrangement is using inline or staggered layout such as semi-circular, delta and dimple vortex generator.

Type IV: Heat sink with loose vortex generator: The enhancements of this category are still vortex generators or dimple/protrusion structure but with sparse arrangement of vortex generator.

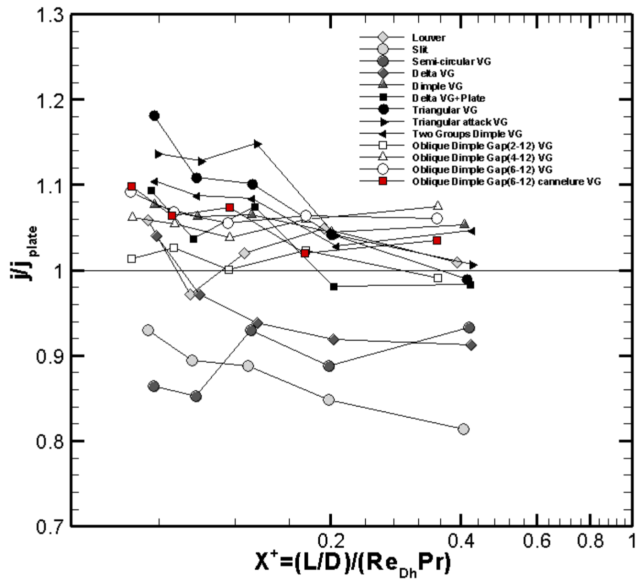

FIG. 5. INVERSE GRAETZ NUMBER X+ VS. j/j_{plain} FOR THE TEST HEAT SINKS.

For a further comparison about the influence of developing flow on the heat transfer performance, test results are plotted in terms of f/f_{plain} and j/j_{plain} vs. the inverse Graetz number as depicted in Figs. 4 and 5. It can be found that the friction factor for interrupted fin geometry is significantly higher than other fin types. And the louver fins show the highest friction factor amid the fin patterns, followed by the dense vortex generator and loose vortex generators. Normally the frictional performance of enhanced fin exceeds that of plain fin geometry except the oblique dimple VG with cannelure structure which shows an appreciable lower pressure drop than that of plain fin geometry. It is interesting to note that f/f_{plain} for the test surfaces can be characterized into three categories, and they are region of heat sink with interrupted fin geometry (Type II) representing the highest friction penalty relative to the plain fin geometry, region of dense vortex generator (Type III) showing moderate increase of pressure drop and region of loose vortex generator (Type IV) with only minor increase of or even lower of pressure drop. In view of the results, it is generally concurred that more complicated fin structure will lead to higher pressure drop. On the other hand, the slope of f/f_{plain} denotes the change of the pressure drop ratio subject to velocity variation. Apparently, the three types of fin patterns reveal completely different characteristics. The slope of Type II is nearly constant throughout test range while the slope of type III is slightly decreased with the Reynolds number; but the slope of type IV remains virtually unchanged as zero. The frictional characteristics of the oblique dimple are nearly the same as that of plain fin geometry. With a further addition of a cannelure structure to the oblique dimple structure leads to a further drop of pressure drop. In fact, the corresponding pressure drop is only 82~85% that of plain fin geometry. Notice that the depth of cannelure structure is about 0.05 mm. Apparently the cannelure structure provides some air tunnels that assist to reduce the entrance loss and the friction loss.

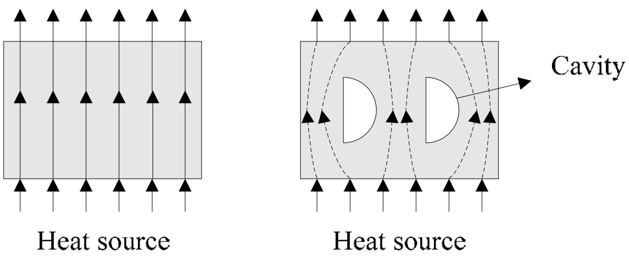

FIG. 6. SCHEMATIC OF THE CONDUCTION PATH WITH AND WITHOUT THE INTERRUPTED BLOCKAGE.

However, the trend of tested results on Colburn *j* factor show that the enhancement of heat transfer does not accord with the frictional characteristics as appeared in Fig. 5. The heat transfer performance for the vortex generators exceed all other fin geometry since it can produce swirl flow, Coanda deflection flow, and destabilized flow field. Nevertheless, the arrangement of vortex generator may cast significant impact on the heat transfer performance. An intensive arrangement of VG offsets the overall heat transfer performance. For example, the heat transfer performance for the Delta VG, semi-circular VG and slit fin geometry are generally lower than that of plain fin geometry. The reasons for this deterioration are two-fold. Firstly, the swirled flow motion engendered by the VGs is only effective when the downstream is less structured. Highly dense VG structure inevitably places blockage to the generated swirled flow. Secondly, these three fin patterns are punched out structure as interrupted surface, thereby blockage of conduction path shown by Figure 6 leads to a further drop of heat transfer performance. With the presence of interrupted configuration like the semi-circular VG, the conduction path is constricted, yielding a performance drop. Note that the louver fin is also a highly interrupted surface but it provide substantial mixing which counterbalance the loss of conduction loss.

A further examination the augmentation level shown in the figure, apparently two regions can be identified; for a lower inverse Graetz number ($x^+ < 0.1$) where the entrance effect plays a significant role, one can see all the less structured VGs show substantial improvements of heat transfer. In fact this is applicable to most the enhanced fin patterns being tested. Among the test fin patterns at $x^+ < 0.1$, the heat transfer performance for heat sink with loose vortex generator (Type IV) outperforms other augmentations. On the other hand, for a fully developed situation where $x^+ > 0.1$, a clear level-off of the enhanced level for all the enhanced fin patterns is seen, and most of the augmentations of interrupted fin geometry (Type II) and dense vortex generator (Type III) fail. The test results suggest that the airside enhancements highly depend upon the arrangement and developing characteristics. Most of the conventional augmentation is effective only in developing regions. Yet in fully developed region, one must seek alternative enhancement using different mechanism of enhancements. In summary of the forgoing discussions, it is found that interrupted fin and dense vortex generators fin are less effective when operated at a lower Reynolds number.

There are some explanations why most of the enhanced fin patterns fail in the fully developed region. The objective of the vortex generator is to provide swirl flow by which better mixing is achieved. However, the formation of longitudinal vortex is constrained when the fin spacing is reduced. The argument of vortex suppression can be found from a 3-D numerical investigation of a plain fin-and-tube heat exchanger performed by Torikoshi et al. [16]. Their investigation showed that the vortex forms behind the tube can be suppressed and the entire flow region can be kept steady and laminar when the fin pitch is rather small. In this sense, it explains part of the reason that the vortex generator is restrained. However, for a very low operation velocity, there is another cause for heat transfer degradation which is the blockage of conduction path of the interrupted surface. With the presence of interrupted configuration like the slit fin and semi-circular VG, the conduction path is constricted, yielding a performance drop. This phenomenon becomes more pronounced when the influence of conduction becomes more eminent. That is why at a frontal velocity of 1 m/s and a fin pitch of 1 mm, the heat transfer coefficient for plain fin exceeds most the fin patterns being tested. In fact, this effect does not occur in dimple VG fin due to continuous conduction path. In summary of the test results, the heat transfer augmentation at $x^+ > 0.1$ is very difficult via conventional interrupted surface (Yang et al. [2]) or via typical vortex generator. A more compromised design is the loose vortex generator (Type IV) design where the resistance at the downstream is lifted, giving more free space for the vortex development. As a consequence, a small enhancement of this design is seen. The test results suggest it would be made possible from different mechanisms, e.g. unstable swing flow or asymmetric fin design.

CONCLUSIONS

The present study conducts an experimental study concerning the airside performance of heat sinks under cross flow condition. The test fin patterns can be classified into four categories, namely the base plain fin heat sink (Type I), interrupted fin geometry (Type II), dense vortex generator (Type III), loose vortex generator (Type IV) and their combinations. It is found that the heat transfer performance is strongly related to the arrangement of enhancements. The interrupted and dense vortex generator configurations normally contribute more pressure drop penalty than improvements of heat transfer. This deterioration becomes especially evident at a lower frontal velocity. There is only one VG – the oblique VG with cannelure structure shows an appreciable lower pressure drop than that of plain fin geometry. Normally the plain fin pattern outperforms most of the enhanced fin patterns of type II and type III at fully developed region. In the meantime, the presence of interrupted surface may also jeopardize heat conduction path due to constriction. The results indicate that the vortex generators operated at a higher frontal velocity is more beneficial than that of plain fin geometry. The results show that at a frontal velocity around 3~5 m/s using fins like triangular, triangular attack and two-groups dimple may be quite effective. In summary of the test results, it is therefore concluded that augmentation via various fin patterns like interrupted or vortex generator is quite effective only at developing region. However, the conventional enhanced fin patterns lose its superiority at the fully developed region. To tackle this problem, some techniques employing swing flow or unstable flow field accompanied with the asymmetric design, shows potential to resolve this problem.

ACKNOWLEDGEMENTS

The authors would like to express gratitude for the supporting funding from the Department of Industrial Technology, Ministry of Economic Affairs, Taiwan.

REFERENCES

[1] Yeh, L. T., 1995, "Review of Heat Transfer Technologies in Electronic Equipment," ASME J. Electronic Packaging **117**, pp. 333－339.

[2] Yang, K. S., Chiang, C. M., Lin, Y. T., Chien, K. H., and Wang, C. C., 2007, "On the Heat Transfer Characteristics of Heat Sinks: Influence of fin spacing at low Reynolds Number Region," Int. J. of Heat and Mass Transfer, **50**, pp. 2667-2674.

[3] Webb, R. L., and Trauger, P., 1991, "Flow Structure in the Louvered fin Heat Exchanger Geometry," Experimental Thermal and Fluid Science, **4**, pp. 205-217.

[4] Davenport, C. J., 1983, "Correlations for Heat Transfer and Flow Friction Characteristics of Louvered Fin," AIChE Symposium Series, **79** (225), pp. 19-27.

[5] Achaichia, A., and Cowell, T. A., 1988, "Heat Transfer and Pressure Drop Characteristics of Flat Tube and Louvered Plate Fin Surface," Experiment Thermal and Fluid Science, **1**, pp. 147-157.

[6] R. K. Shah, D.P. Sekulić, Heat Exchangers, in Handbook of Heat Transfer, edited by W. M. Rohsenow, J.P. Harnett, and Y.I. Cho, J.P. chapter 17, p. 17.70, McGraw-Hill, New York, 1998.

[7] Sergent, J. E., and Krum, A., 1998, *Thermal Management Handbook for Electronic Assemblies*, McGraw-Hill, New York.

[8] Fiebig, M., 1995, "Embedded Vortices in Internal Flow: Heat Transfer and Pressure Loss Enhancement," Int. J. Heat Fluid Flow, **16**, pp. 376–388.

[9] Schubauer, G. B., and Spangenberg, W. G., 1960, "Forced Mixing in Boundary Layers," J. Fluid Mech., **8**, pp. 10-31.

[10] Fiebig, M., Kallweit, P., and Mitra, N. K., 1986, "Wing Type Vortex Generators for Heat Transfer Enhancement," *Proc. Eighth Int. Heat Transfer Conf.*, **6**, pp. 2909-2913.

[11] Fiebig, M., Kallweit, P., Mitra N.K., and Tiggelbeck, S., 1991, "Heat Transfer Enhancement and Drag by Longitudinal Vortex Generators in Channel Flow," Exp. Thermal Fluid Sci., **4**, pp. 103-114.

[12] Tanaka, T., Itoh, M., Hatada, T., and Matsushima, H., 2003, "Influence of Inclination Angle, Attack Angle, and Arrangement of Rectangular Vortex Generators on Heat Transfer Performance," Heat transfer – Asian Research, **32**, pp. 253-267.

[13] ASHRAE Handbook Fundamental. SI-Edition, American Society of Heating, Refrigerating and air-conditioning Engineers, Inc., Atlanta, 1993, pp. 13.14-13.15.

[14] ASHRAE Standard 41.2-1987, Standard Methods for Laboratory Air-flow Measurement, American Society of Heating, Refrigerating and Air-Conditioning Engineers, Inc., Atlanta, 1987.

[15] Moffat, R. J., 1988, "Describing the Uncertainties in Experimental Results," Exp. Thermal and Fluid Sci., **1,** pp. 3-17.

[16] Torikoshi, K., Xi, G., Nakazawa, Y., and Asano, H., 1994, "Flow and Heat Transfer Performance of a Plate-fin and Tube Heat Exchanger (1st Report: Effect of Fin Pitch)," in *Proceedings of the 10th Int. Heat Transfer Conf.*, paper 9-HE-16, pp. 411-416.

ACKNOWLEDGMENTS

The author is indebted to the financial support (99-2218-E-009-012-MY2) from the National Science Council, Taiwan.